Manganese Deficiency Leads to Genotype-Specific Changes in Fluorescence Induction Kinetics and State Transitions[1][C][OA]

Søren Husted*, Kristian H. Laursen, Christopher A. Hebbern, Sidsel B. Schmidt, Pai Pedas, Anna Haldrup, and Poul E. Jensen

Plant and Soil Science Laboratory, Department of Agriculture and Ecology (S.H., K.H.L., C.A.H., S.B.S., P.P.), and The Villum Kann Rasmussen Research Center "Pro-Active Plants," Department of Plant Biology and Biotechnology, Faculty of Life Sciences, University of Copenhagen, DK–1871 Frederiksberg C, Copenhagen, Denmark (A.H., P.E.J.)

Barley (*Hordeum vulgare*) genotypes display a marked difference in their ability to tolerate growth at low manganese (Mn) concentrations, a phenomenon designated as differential Mn efficiency. Induction of Mn deficiency in two genotypes differing in Mn efficiency led to a decline in the quantum yield efficiency for both, although faster in the Mn-inefficient genotype. Leaf tissue and thylakoid Mn concentrations were reduced under Mn deficiency, but no difference between genotypes was observed and no visual Mn deficiency symptoms were developed. Analysis of the fluorescence induction kinetics revealed that in addition to the usual O-J-I-P steps, clear K and D steps were developed in the Mn-inefficient genotype under Mn deficiency. These marked changes indicated damages to photosystem II (PSII). This was further substantiated by state transition measurements, indicating that the ability of plants to redistribute excitation energy was reduced. The percentage change in state transitions for control plants with normal Mn supply of both genotypes was 9% to 11%. However, in Mn-deficient leaves of the Mn-inefficient genotypes, state transitions were reduced to less than 1%, whereas no change was observed for the Mn-efficient genotypes. Immunoblotting and the chlorophyll *a/b* ratio confirmed that Mn deficiency in general resulted in a significant reduction in abundance of PSII reaction centers relative to the peripheral antenna. In addition, PSII appeared to be significantly more affected by Mn limitation than PSI. However, the striking genotypic differences observed in Mn-deficient plants, when analyzing state transitions and fluorescence induction kinetics, could not be correlated with specific changes in photosystem proteins. Thus, there is no simple linkage between protein expression and the differential reduction in state transition and fluorescence induction kinetics observed for the genotypes under Mn deficiency.

Manganese (Mn) deficiency is a major plant nutritional disorder, often caused by an alkaline soil pH, which favors oxidation of soluble Mn^{2+} to the plant-unavailable form MnO_2. Mn-deficient crops are found in many areas of the world but are especially widespread in Australia, the United States, Asia, and northern Europe, including Scandinavia. A recent survey estimated that approximately 30% of soils in China are Mn deficient, causing severe yield and quality reductions in crops (Yang et al., 2007). Likewise, Mn deficiency has become the foremost plant nutritional problem in major parts of Scandinavia (Hebbern et al., 2005, 2009).

The oxygen-evolving complex (OEC) in PSII has a metalloenzyme core containing both Mn^{2+} and Ca^{2+} ions as well as the halogen ion Cl^- (Kok et al., 1970). The reaction center protein PsbA (D1) binds the inorganic core, which has the empirical formula $Mn_4Ca_1O_xCl_{1\text{-}2}(HCO_3)_y$ and is known as the tetra-nuclear Mn cluster (Dasgupta et al., 2008). More than 80% of all Mn contained in the chloroplasts is associated with PSII (Anderson et al., 1964). Thus, Mn deficiency leads to a rapid reduction in oxygen production (Andersson and Pyliotis, 1969; Nable et al., 1984; Chatterjee et al., 1994) and to a marked change in chlorophyll (Chl) *a* fluorescence induction kinetics (Anderson and Thorne, 1968; Kriedemann et al., 1985). Continuous Mn deficiency is followed by the development of characteristic visual leaf symptoms such as intravenous chlorosis and subsequently the development of necrotic spots, which are supposed to be related to disorganization of the thylakoid system and loss of PSII reaction centers (Simpson and Robinson, 1984; Papadakis et al., 2007). Photoinhibition-induced impairment of the OEC leads to accumulation of highly oxidized species such as $P680^+$, which might lead to the generation of singlet oxygen and subsequent oxidation of the local protein

[1] This work was supported by the Ministry of Science, Technology, and Innovation (contract nos. 53–00–0234 and 274–06–0325), the Danish Grain Breeding Foundation, the Danish National Research Foundation, the Villum Kann Rasmussen Foundation, and the Danish Natural Science Research Council (contract no. 272–05–0360).

* Corresponding author; e-mail shu@life.ku.dk.

The author responsible for distribution of materials integral to the findings presented in this article in accordance with the policy described in the Instructions for Authors (www.plantphysiol.org) is: Søren Husted (shu@life.ku.dk).

[C] Some figures in this article are displayed in color online but in black and white in the print edition.

[OA] Open Access articles can be viewed online without a subscription.

www.plantphysiol.org/cgi/doi/10.1104/pp.108.134601

environment, thereby promoting the degradation of core proteins in the PSII reaction center (Apel and Hirt, 2004; Møller et al., 2007). Krieger and coworkers (1998) demonstrated that successive depletion of Ca^{2+}, Cl^{-}, or Mn^{2+} in OEC from spinach (*Spinacia oleracea*) resulted in the strongest reduction in PSII activity when Mn was depleted, being closely related to degradation of PsbA. A repair cycle operates to replace the damaged subunits of PSII, especially PsbA (Aro et al., 1993, 2005; Nixon et al., 2004), and it has been estimated that the half-life of PsbA in the light is just a few minutes, depending on the Chl concentration (He and Vermaas, 1998).

Genotypes of winter barley (*Hordeum vulgare*) are known to respond differently to low Mn availability (Hebbern et al., 2005), a phenomenon commonly referred to as differential Mn efficiency (Ascher-Ellis et al., 2001). Mn deficiency can be controlled using Mn-efficient genotypes during moderate Mn limitation (Hebbern et al., 2005). However, the underlying physiological mechanisms are still incompletely understood, despite the fact that numerous studies have been initiated to examine the issue during the last decades. Exudation of MnO_2-reducing root exudates (Bromfield, 1958; Hannam et al., 1985; Rengel, 1997) and a more efficient translocation of Mn between roots and shoot in Mn-efficient genotypes (Pearson and Rengel, 1997) have been suggested, but clear experimental evidence is still lacking. Pedas and coworkers (2005) identified a high-affinity uptake system for Mn^{2+} in barley, operating at concentrations below 150 nM, and demonstrated that Mn-efficient genotypes assimilated Mn^{2+} with a higher affinity and four times the rate of Mn-inefficient genotypes. Moreover, it was found that Mn efficiency in barley genotypes correlated with the expression level of the root plasma membrane-localized Mn transport protein HvIRT1 (Pedas et al., 2008). This more efficient uptake system was followed by a rapid translocation of Mn to the growing meristem and is consequently believed to be an important parameter in differential Mn efficiency among barley genotypes.

Despite the fact that Mn is a key component of PSII, there have not been any previous attempts to examine the relationship between differential Mn efficiency and the resistance of the photosynthetic apparatus to perturbations induced by Mn deficiency. Thus, this study was undertaken in order to identify genotypic differences in the energy transfer within the PSII reaction center that may correlate with Mn efficiency. The genotypic differences were investigated by pulse amplitude-modulated fluorescence, analysis of the fluorescence induction kinetics, and selected PSII and PSI components.

RESULTS

Plant Growth under Mn Deficiency

The development of visible leaf symptoms caused by Mn deficiency could be prevented if the quantum yield efficiency of PSII (F_v/F_m) on dark-adapted leaves was kept above 0.55 for a period of at least 4 weeks under the conditions given (data not shown). Thus, the intensity of Mn deficiency in plants was followed and controlled by measuring F_v/F_m throughout the experimental period (Fig. 1A). Control plants were successfully maintained at F_v/F_m values close to the theoretical optimum of 0.83 (Björkman and Demmig, 1987) for both genotypes throughout the experiment. However, 13 d after induction of Mn deficiency, a decline in F_v/F_m in the Mn-deficient plants could be observed (Fig. 1A). This decline was most pronounced in the Mn-inefficient genotype Antonia, while the Mn-efficient Vanessa was less responsive to Mn deficiency. At 32 d after induction of Mn deficiency, the F_v/F_m threshold value of 0.55 was approached; consequently, the weekly additions of Mn were raised (see "Materials and Methods") in order to maintain Mn deficiency at a fairly constant F_v/F_m ratio of 0.6 ± 0.05 (Fig.

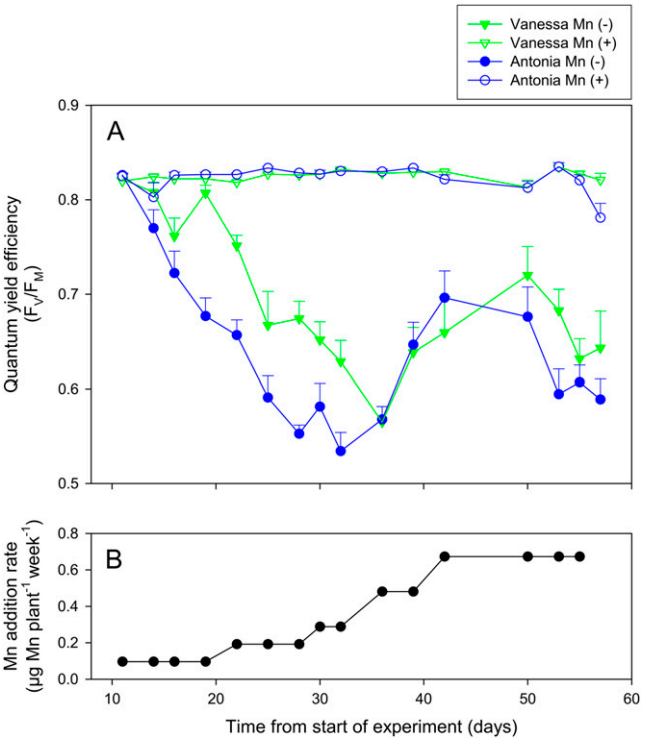

Figure 1. A, F_v/F_m of the Mn-efficient genotype Vanessa and the inefficient genotype Antonia with ample Mn supply or exposed to Mn deficiency. B, The weekly total Mn supply to plants exposed to Mn deficiency. Plants were precultivated for 1 week with ample supply of all essential nutrients followed by splitting into two groups, either maintained at an ample nutrient supply [control; Mn(+)] or transferred to a Mn-depleted nutrient solution [Mn(−)]. In order to induce Mn deficiency without development of leaf symptoms, F_v/F_m was maintained above 0.55 by addition of 100 to 650 ng of Mn per plant per week, depending on the growth stage, whereas the control received 10 times this dosage. Each data point represents the mean ± SE ($n = 8$). [See online article for color version of this figure.]

1). Using this strategy, no visual differences between the controls and Mn-deficient plants were observed throughout the experimental period.

Mn Content in Leaf Tissue and Thylakoids

The Mn concentration was analyzed in the youngest fully expanded leaf 44 and 50 d after the induction of Mn deficiency (Fig. 2), and the Mn concentration of thylakoids was analyzed prior to termination of the experiment. These results supported that the low F_v/F_m values were caused by Mn deficiency. The Mn concentration in the thylakoids of the inefficient genotype was reduced from 0.75 ± 0.03 to 0.48 ± 0.10 mg Mn g^{-1} Chl under Mn deficiency, whereas the similar values for the efficient line were a reduction from 0.88 ± 0.09 to 0.61 ± 0.02 mg Mn g^{-1} Chl. Thus, clearly less Mn was found in the thylakoids of Mn-deficient plants, but no significant difference was found between the genotypes. Likewise, the Mn concentrations in leaves from deficient plants were significantly below the critical threshold concentrations of 17 μg Mn g^{-1} dry weight for both barley genotypes (Reuter et al., 1997). However, there were no significant differences in leaf tissue Mn concentrations between the genotypes in either the Mn deficiency treatment or the control treatment (Fig. 2). Furthermore, the multielemental analysis also confirmed that the plants were not suffering from any other nutrient deficiencies than Mn when comparing data with nutrient deficiency threshold limits presented by Reuter and coworkers (1997; data not shown).

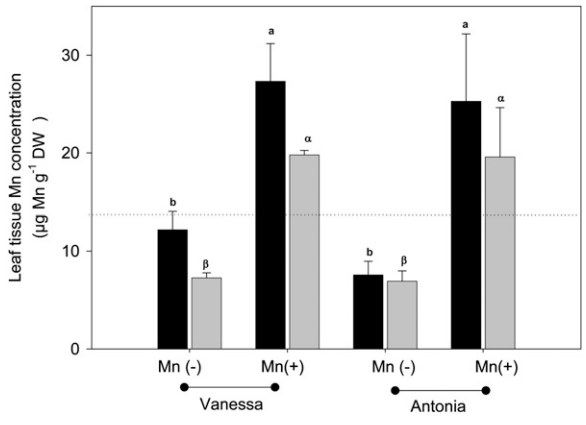

Figure 2. Mn concentrations in leaf tissue for the Mn-efficient genotype Vanessa and the Mn-inefficient genotype Antonia measured 44 d (black bars) and 50 d (gray bars) after planting, respectively. Mn(+) and Mn(−) indicate the Mn sufficiency and deficiency treatments, respectively. The critical threshold concentration for Mn in leaf tissue (17 μg Mn g^{-1} dry weight [DW]) is indicated by the dotted line (Reuter et al., 1997). Means ± SE ($n = 3$) with the same letter at each date are not significantly different.

Mn Deficiency Leads to the Development of K and D Steps in the Chl *a* Fluorescence Induction Curves

Besides reducing the F_v/F_m value, Mn deficiency introduced a number of distinct changes in the position of the O-J-I-P steps and the general shape of the Chl *a* fluorescence induction curves (Fig. 3). When the degree of Mn deficiency intensified and the F_v/F_m value was reduced below 0.67, a new step at 0.2 to 0.4 ms appeared in the fluorescence induction curves, designated as the K step by Strasser et al. (2004). This was accompanied by an additional and pronounced decline later in the curve, after the I step at 75 to 90 ms, designated as the D step by Strasser et al. (1995). The measurements on Mn-deficient leaves from the genotype Antonia showed the greatest changes in the curves, representing a more extreme Mn-deficient condition than was the case with Vanessa. It is important to note that the shape of the fluorescence induction curves with similar F_v/F_m values differed markedly between Antonia and Vanessa (e.g. compare curves 3 and 4 in Fig. 3), indicating that more severe disturbances of the photosystems took place in the inefficient relative to the efficient genotype.

State Transitions

Plants have the ability to adjust the energy input to PSII and PSI by moving a mobile pool of the light-harvesting complex (LHCII) proteins (Lhcb1, Lhcb2, and Lhcb3) between the photosystems by a state transition process. The mobility of LHCII between photosystems is controlled by phosphorylation (Bellafiore et al., 2005). When LHCII is bound to PSII, plants are in state 1, and when LHCII is associated with PSI, they are in state 2 (for review, see Haldrup et al., 2001). State transitions were determined 38 and 50 d after induction of Mn deficiency with similar results (Fig. 4). It is clearly seen that the baseline fluorescence was stable and that no significant curvature occurred over time, indicating stable analytical conditions and accurate state transition measurements. When performing the state transition analysis, it was repeatedly noted that the background fluorescence level in Mn-deficient leaves was more than doubled relative to the control (Fig. 4, compare A and B), which indicates an increased fluorescence emission from detached antenna proteins.

In the control plants (Fig. 4A), the maximum fluorescence in state 1 (F_{m1}) was clearly higher than in state 2 (F_{m2}), indicating that the ability to adjust to PSI and PSII light was intact. The percentage change in state transitions $[(F_{m1} - F_{m2})/F_{m1}]$ was measured to 9% to 11% in healthy control plants and was not significantly different between the control samples of both genotypes (Fig. 5A). In Figure 4B, the effect of Mn deficiency on state transition in the Mn-inefficient genotype Antonia is illustrated, and it is clearly seen that the ability to perform state transitions has been reduced significantly. The percentage change in state

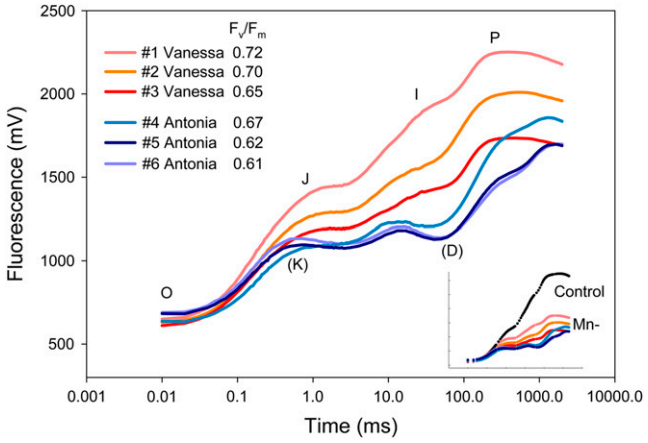

Figure 3. Fluorescence induction kinetics from Mn-deficient leaves of Mn-efficient Vanessa and Mn-inefficient Antonia measured 57 d after planting. The individual phases of the transient are designated O-J-I-P. When F_v/F_m decreased below 0.67 in the Mn-inefficient genotype Antonia, the slope of the transients became negative at two distinct points, 0.2 to 0.4 ms and 75 to 90 ms, and these additional steps were designated as the K and D steps, respectively (notice logarithmic *x* axis). Inset, A fluorescence transient from a control leaf relative to all of the Mn-deficient (Mn−) measurements shown in the main figure.

transition for Mn-deficient leaves was reduced to less than 1% of the Mn-inefficient genotype Antonia, whereas Mn deficiency did not cause any significant effect on state transitions in the Mn-efficient genotype Vanessa (Fig. 5A).

The F_v/F_m was determined immediately before the state transition experiments, and despite a striking difference in the ability to perform state transitions, at both 38 and 50 d after Mn deficiency induction, no significant differences in F_v/F_m values between Mn-deficient Vanessa and Antonia were observed on both occasions (Fig. 1A).

Immunoblotting showed that there was no significant difference in the amount of Lhcb1 between control and Mn-deficient leaves, but a marked decrease in the phosphorylated form of LHCII (P-Lhcb1 and P-Lhcb2) was observed when plants were exposed to Mn deficiency (Fig. 5B). Likewise, a significant reduction in the Chl *a* concentration was observed in Mn-deficient plants, whereas the Chl *b* concentration remained stable (Fig. 5C). The Chl measurements suggest a significant reduction in the amount of functional PSII reaction centers relative to the peripheral antenna under Mn deficiency, which subsequently was confirmed by the immunoblot-based quantification of PsbA (Fig. 5D). Generally, Mn deficiency led to a 75% reduction in the amount of PsbA (representing PSII), whereas PSI-F (representing PSI) under the same conditions was reduced to approximately 45% in both genotypes. Time of analysis is a very important parameter to consider when nutrient deficiency studies are undertaken, as the impact of the physiological perturbations change with age and intensity of the deficiency. However, those trends described above were found to be highly consistent and were confirmed by repeating parts of the experiments several times using plants of different physiological age and severity of Mn deficiency (data not shown). Thus, Mn deficiency resulted in a clear preferential degradation of the PSII reaction centers relative to PSI. However, it is important to note that no significant genotypic effects in the composition of reaction centers and antenna proteins could be observed, and apparently there is no simple linkage between protein expression and the differential reduction in state transition observed for Antonia under Mn deficiency (Fig. 5, compare A with B–D).

Nonphotochemical Quenching

Nonphotochemical quenching (NPQ) protects PSII from photoinhibition and was determined under light intensities equivalent to growth light (Table I). When plants were exposed to Mn deficiency in growth light, NPQ was reduced by 53% in the Mn-inefficient genotype Antonia and by 38% in the Mn-efficient genotype

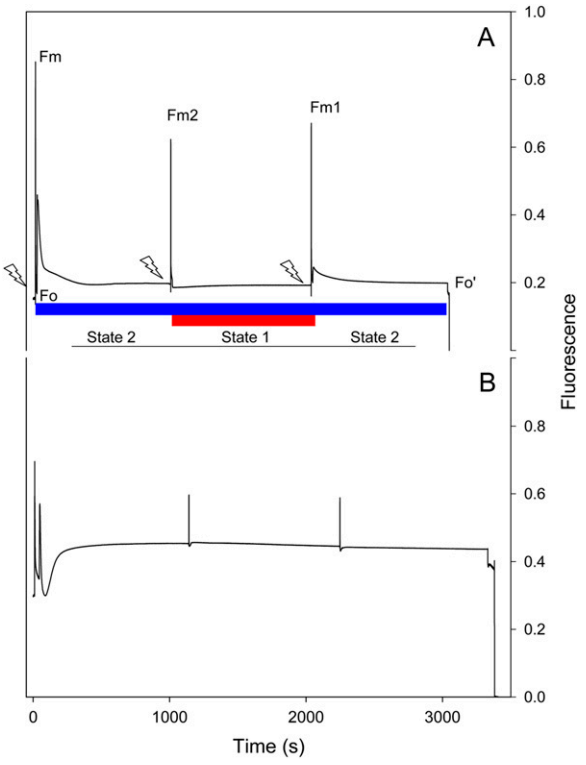

Figure 4. State transitions in the Mn-inefficient genotype Antonia measured 38 d after planting for control (A) and Mn-deficient (B) plants. Dark-adapted leaves were exposed to blue and red light preferentially exciting PSII (state 2) or PSI (state 1), respectively. State 2 was induced by illuminating the detached leaf for 20 min with blue light, and F_{m2} was determined after a saturating light pulse. Red light was then added, and after 20 min, F_{m1} was determined after a saturating light pulse. F_0 and F_m are the initial minimum and maximum PSII fluorescence levels in darkness, and F_0' is the fluorescence minimum in light. Saturating white light pulses are indicated by arrows. [See online article for color version of this figure.]

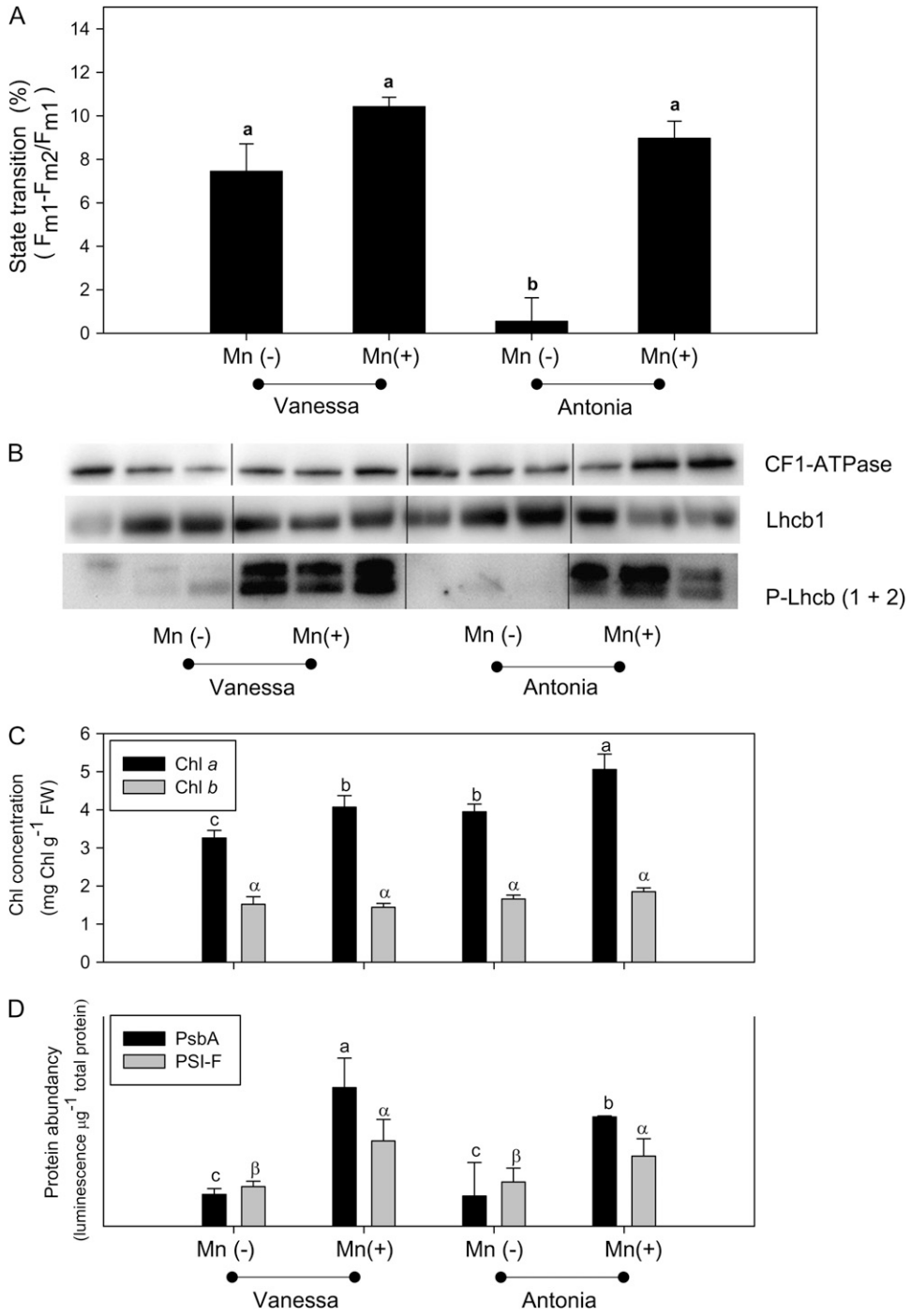

Figure 5. A, State transition in Mn-efficient (Vanessa) and Mn-inefficient (Antonia) genotypes under control and Mn-deficient conditions measured 55 d after planting. The percentage state transition was calculated using the difference in peak height of maximal fluorescence following a saturating pulse in state 1 and state 2 ($F_{m1} - F_{m2}/F_{m1}$). Values are means ± SE (n = 3). Bars with the same letter were not significantly different. B, Immunoblotting of unphosphorylated (Lhcb1) and phosphorylated (Lhcb1 + Lhcb2) light-harvesting protein when the Mn-efficient (Vanessa) and Mn-inefficient (Antonia) genotypes were exposed to control and Mn-deficient conditions. Three individual preparations of thylakoid proteins from each combination of cultivar and treatment are shown. CF1-ATPase was included as a loading control. C, Chl *a* and *b* concentrations per gram fresh weight (FW) of the youngest fully expanded leaf in Mn-efficient (Vanessa) and Mn-inefficient (Antonia) genotypes exposed to control and Mn-deficient conditions. Values are means ± SE (n = 4). Bars with the same letter were not significantly different. D, Immunoblotting of PsbA and PSI-F representing PSII and PSI, respectively. The protein abundance was quantified using chemiluminescence and expressed per unit of total protein loaded. Values are means ± SE (n = 4). Bars with the same letter were not significantly different.

Vanessa. In addition, a marked reduction in quantum yield of PSII (ϕ_{PSII}) was also observed, describing a loss of photochemical efficiency in the Mn-deficient leaves. The PSII excitation pressure (1-q_P) is an approximation of the relative fraction of reduced PSII (Rosenqvist and van Koten, 2003). There was no significant difference in 1-qP between the control and Mn deficiency treatments for the Mn-inefficient genotype Antonia. In contrast, a significant increase in 1-q_P of 26% in the Mn-efficient genotype was observed when Mn-deficient and Mn-sufficient Vanessa plants were compared. Thus, it appears that Mn deficiency hampers the ability of the Mn-inefficient genotype Antonia to reduce the plastoquinone pool (PQ) of PSII, whereas this ability is significantly less affected in the Mn-efficient genotype Vanessa. These findings are in good agreement with the poor ability of Antonia to perform state transitions (Fig. 5A).

Table I. *ϕ_{PSII}, 1-q_P, and NPQ measured in growth light 46 d after induction of Mn deficiency*

Mean values ± SE ($n = 3$ for control plants and $n = 6$ for Mn-deficient plants) for each parameter marked with the same letter were not significantly different.

Genotype	Treatment	ϕPSII	1-qP	NPQ
Vanessa	−Mn	0.44 ± 0.05b	0.24 ± 0.02a	0.41 ± 0.05b
	Control	0.56 ± 0.01a	0.19 ± 0.01b	0.66 ± 0.04a
Antonia	−Mn	0.41 ± 0.05b	0.19 ± 0.03b	0.29 ± 0.07c
	Control	0.53 ± 0.05a	0.21 ± 0.04b	0.61 ± 0.04a

DISCUSSION

The Chl *a* Fluorescence Induction Curve for Mn-Deficient Plants

The leaf tissue concentration of Mn was clearly reduced below the critical threshold limit for Mn deficiency in barley plants in both the Mn-efficient genotype Vanessa and the Mn-inefficient genotype Antonia. Likewise, the induction of Mn deficiency resulted in a similar decrease in thylakoid Mn concentrations for both genotypes, but surprisingly, no difference in Mn concentrations was observed between the two genotypes (Fig. 2). However, the induction of Mn deficiency resulted in a number of marked changes to the Chl *a* fluorescence induction curves (Fig. 3). Especially, it should be noted that Mn deficiency resulted in marked differences between genotypes, at the same Mn tissue concentration, when the Chl *a* fluorescence induction curves were compared (Fig. 3). Thus, analysis of Chl *a* fluorescence induction curves as well as state transition results might constitute a powerful tool to diagnose Mn deficiency in plants well before it can be diagnosed visually.

In addition to the typical O-J-I-P steps on the fluorescence induction curves, the development of a clear K step at 0.2 to 0.4 ms was noticed in Antonia. The K step has previously been reported to be induced by heat stress (Srivastava et al., 1997; Strasser, 1997). The K step was not developed in Vanessa, where the F_v/F_m values indicated that Mn deficiency was not as strongly induced as for Antonia (Fig. 1). The physiology behind the development of a K step is not fully understood, but generally it is assumed that the appearance of the K step reflects damages to the OEC (Strasser, 1997; Lazar, 2006). In our measurements, the clear development of a K step most likely represented an extreme of Mn deficiency in the leaf. Nonetheless, the interpretation of the K step as an indicator of damage to the OEC (Bukhov et al., 2004) is consistent with the observation that Mn deficiency exerted major disturbances in the protein composition of PSII (Fig. 5).

The second notable feature of the fluorescence induction curves from Mn-deficient Antonia was the appearance of a decline in the curve after the I step (Fig. 3), creating a so-called D step at 75 to 90 ms (Munday and Govindjee, 1969). This phase has previously been attributed to an additional reduction of PQ_A, as both PQ_A and PQ_B become further reduced (Strasser et al., 1995; Hill et al., 2004), but generally, very little is known about this additional step on the Chl *a* fluorescence induction curve.

Mn-Deficient Plants Lose the Ability to Perform State Transitions

The loss of adaptive mechanisms that optimize photosynthetic performance under varying light conditions or leading to diminished photoprotection may provide a mechanistic cause for a significant fraction of the grain yield reduction that occurs when barley plants are exposed to Mn deficiency. State transitions are considered to be one such adaptive mechanism. When PSII is favored over PSI, then excitation energy may be redistributed to PSI by changing the redox state of the thylakoids. A reduced pool of PQ is bound to the cytochrome b_6f complex and activates a LHCII kinase, which phosphorylates Lhcb1 and Lhcb2 proteins and detaches a fraction of LHCII from PSII. Consequently, this LHCII migrates from PSII to PSI, leading to a preferential excitation of PSI and a rebalancing of light energy absorption between the two photosystems (Allen et al., 1981; Haldrup et al., 2001). There is evidence that growth under low light requires state transitions in order for the plant to optimize light harvesting and minimize light stress (Mullineaux and Emlyn-Jones, 2004). However, state transitions appear to be important under varying growth conditions and less important under controlled conditions (Lunde et al., 2000).

The ability to perform state transitions was highly reduced in the Mn-inefficient genotype Antonia when exposed to Mn deficiency (Figs. 4 and 5A). The difference in state transitions between Mn-deficient genotypes is in good agreement with the observation that Mn-deficient plants and especially the Mn-inefficient genotype Antonia are less efficient at generating a reduced PQ pool, as approximated by the redox state of the PQ pool (1-qP; Table I), thereby initiating the redox-controlled phosphorylation of LHCII. However, the loss of state transitions in Antonia was apparently not due to a loss of light-harvesting complexes (Fig. 5B). Immunoblotting revealed no significant reductions in Lchb1 in the Mn-deficient samples and likewise no difference between the genotypes (Fig. 5B). However, detection of the phosphorylation levels of P-Lhcb1 and P-Lhcb2 showed a marked reduction in both genotypes

under Mn deficiency (Fig. 5B), and clearly, no correlation between the amount of phosphorylated protein and the ability to perform state transitions could be observed. It appears that the observed difference in state transition might be influenced by (1) other proteins of the PSII reaction centers or antenna, (2) differential posttranslational modification of proteins expressed in equal amounts in the genotypes, or (3) specific changes in protein conformation.

Fluorescence Quenching Parameters

NPQ declined by 40% to 50% in Mn-deficient plants, reflecting a situation where the donor side of PSII was under increased stress but the mechanisms of photoprotection had not been up-regulated (Table I). Marked reductions in ϕ_{PSII} were also observed, indicating a loss of photochemical efficiency in the Mn-deficient leaves of up to 40%. NPQ is considered to be primarily governed by the xanthophyll cycle (Niyogi et al., 2001), while state transitions and photoinhibition represent a smaller component of the total NPQ (Krause and Weis, 1991). Loss of NPQ as a result of Mn deficiency has previously been reported and attributed to a down-regulation of the xanthophyll cycle (Jiang et al., 2002). A translumenal pH gradient is required to initiate and drive the xanthophyll cycle (Muller et al. 2001), and the loss of functional PSII, as in the case of Mn deficiency, would prevent the formation and maintenance of a translumenal pH gradient and thereby reduce NPQ, as observed in this study (Table I). The reduction in NPQ will subsequently lead to photoinhibition, which over time increases the production of reactive oxygen species and promotes PsbA degradation (Barber, 2004). Interestingly, Krieger and coworkers (1998) proposed that Mn has the ability to protect PsbA from oxidative degradation by maintaining a protein structure that is not accessible to cleavage; consequently, it should follow that Mn deficiency leads to OEC degradation, which is in accordance with the observation made in Figure 5D. Loss of OEC leads to a reduced electron transport and a lowering of the fluorescence maximum yield (F_m; Fig. 3, inset). Likewise, Mn deficiency-induced OEC degradation should lead to an increased pool of detached LHCII, which cannot distribute the excitation energy, resulting in increased background fluorescence (F_0), as observed in both the fluorescence induction kinetics and state transition measurements (Figs. 3 and 4). This finding is supported by Jiang et al. (2002), who found that F_0 was almost doubled when maize (*Zea mays*) plants were exposed to severe Mn deficiency, with visual leaf symptoms.

CONCLUSION

The increased vulnerability of the Mn-inefficient genotype Antonia to Mn limitation appears to be influenced by photochemical disturbances. When the two genotypes were supplied equally with low additions of Mn, the leaf tissue and thylakoid concentrations were similar. However, the Chl *a* fluorescence induction curves were markedly different between the genotypes, and the inefficient genotype Antonia had a reduced ability to perform state transitions, whereas the energy transduction in the efficient genotypes was much less affected. This observation might reflect a higher requirement for Mn in photosynthesis for Antonia, so that Mn becomes rate limiting at a higher physiological Mn concentration than in Vanessa. Alternatively, differences in the PsbA repair cycle, such as timely resupply of Mn to the photosystems, or differences in photoprotective mechanisms and susceptibility to damage from oxidative stress may also be important processes. These topics require further analysis.

The results presented in this paper are consistent with Mn deficiency primarily targeting the OEC and affecting the donor side of PSII. Perturbations in the photosynthetic apparatus clearly involved a markedly reduced efficiency of PSII under Mn deficiency due to loss of the PSII core protein (PsbA). Thus, it can be concluded that even mild Mn deficiency without any distinct leaf symptoms may induce damages to PSII and consequently limit harvest yields, adaptability, and survivability of plants under field conditions.

MATERIALS AND METHODS

Cultivation of Plants

Barley (*Hordeum vulgare*) was cultivated hydroponically in 4-L buckets, with four plants in each bucket. Seedlings were germinated on vermiculite, washed with distilled water, and then transferred to hydroponics. The composition of the nutrient solution has been described elsewhere (Husted et al., 2000). The nutrient solutions containing the macronutrients were purified for traces of cationic micronutrients by solid-phase extraction using Chelex-100 resin (Sigma-Aldrich) prior to use (Pedas et al., 2005). Filtered air was provided through steel medical needles suspended in the nutrient solution. All solutions were replaced weekly. The plants were grown in a greenhouse with light provided on a 16-h/8-h day/night cycle at 300 μmol photons m^{-2} s^{-1}. Each treatment was replicated at least three times.

Barley genotypes with contrasting Mn efficiency (Mn-inefficient Antonia and Mn-efficient Vanessa) were precultivated for 1 week with ample supply of all essential nutrients. For the following 7 weeks, plants were split in two groups, either maintained at an ample nutrient supply (control) or transferred to a Mn-depleted nutrient solution. In order to induce Mn deficiency without development of leaf symptoms, 100 to 650 ng of Mn was added per plant per week, depending on the growth stage, whereas the control received 10 times this dosage. Additions of Mn to the nutrient solution and pH adjustment (pH 5.5–6.0) were made on a daily basis in order to limit the effects of a rapid and complete depletion of Mn when given as one weekly addition. This principle of daily additions ensured a more constant supply of Mn to the plants in both the low and control treatments.

Chl *a* Fluorescence Measurements

Measurements of Chl *a* fluorescence were made using a hand-held portable fluorescence detector (Handy Plant Efficiency Analyser; Hansatech Instruments) to determine the maximum F_v/F_m. The leaves were dark-adapted for 30 min using leaf clips before measurement. Fluorescence measurements were recorded by illumination for 2 s with 3,000 μmol photons m^{-2} s^{-1} at a wavelength of 650 nm. The JIP test (Strasser et al., 2004) was performed using Biolyzer software (R. Rodriguez and R. Strasser, University of Geneva).

Isolation of Thylakoid Membranes

Thylakoid membrane isolations were made on approximately 1 g of leaf material from each bucket. Only the youngest, fully emerged leaves were used. Extractions were performed in the cold (5°C) under dimmed green light in order to maintain the integrity of the thylakoids. For homogenization, leaf material was transferred to a 50-mL Falcon tube with 30 mL of homogenizing buffer containing 0.4 M Suc, 10 mM NaCl, 5 mM $MgCl_2$, 20 mM Tricine (pH 7.5), and 10 mM L-ascorbate. Samples were homogenized on an Ultra Turrax T25 (IKA) and then strained through Miracloth (pore size = 22–25 μm; Calbiochem). The extracts were centrifuged for 10 min at 5,000*g*, the supernatant was removed, and the pellet was resuspended in 5 mM Tricine (pH 7.9) and allowed to stand for 15 min in the dark in order to lyse the chloroplasts. Following lysis, the thylakoids were pelleted by centrifugation for 10 min at 12,000*g*, and the pellet was resuspended in a solution containing 0.4 M Suc, 10 mM NaCl, 5 mM $MgCl_2$, 20 mM Tricine (pH 7.9), and 20% glycerol. NaF was added to all of the reagents at a final concentration of 10 mM as a phosphatase inhibitor. The samples were frozen immediately in liquid N_2 and stored at −80°C until further analysis. The samples were stable for at least 3 months.

Inductively Coupled Plasma-Mass Spectrometry Analysis

Leaf tissues of the youngest fully expanded leaf and thylakoid membranes were analyzed for elemental content with inductively coupled plasma-mass spectrometry (ICP-MS; model 7500ce; Agilent Technologies). Leaf samples were freeze dried using a Christ Alpha Freeze Drier (Martin Christ). Approximately 0.2 g of freeze-dried leaf was digested using 70 mL of polyethylene high-density vials (Capitol Vial) on a graphite heating block (Mod Block; CPI International). A modification of the Environmental Protection Agency method 3050 B was used, as described previously (Husted et al., 2004). Accuracy of the ICP-MS analysis was determined using apple (*Malus domestica*) leaf certified reference material (standard reference material 1515; National Institute of Standards and Technology). Data from the ICP-MS was accepted when accuracy was higher than 90% of the value of the certified reference material. Before digestion of thylakoids, 2 mL of thylakoid membrane extraction was freeze dried, followed by removal of the glycerol fraction in a muffle furnace at 500°C. When completely incinerated, samples were dissolved in 5% subboiled HNO_3 and centrifuged two times prior to analysis.

Fluorescence Quenching Analysis and State Transition Measurements

NPQ, maximum ϕ_{PSII}, 1-q_P, and state transitions were measured 6 weeks after induction of Mn deficiency with a pulse amplitude modulation 101-103 fluorometer (Walz), as reported previously (Lunde et al., 2003).

The fluorescence parameters (NPQ, 1-q_P, and Φ_{PSII}) were calculated using the following equations: $1\text{-}q_P = (F_s - F_0')/(F_m' - F_0')$, $\Phi_{PSII} = (F_m' - F_s)/F_m'$, and $NPQ = (F_m - F_m')/F_m'$, where F_s is the steady-state fluorescence, F_m and F_m' are maximum fluorescence induced by an 800-ms saturating actinic light flash (6,000 μmol photons m^{-2} s^{-1}) of dark and preilluminated leaves, respectively, and F_0 and F_0' are fluorescence without illumination of dark-adapted and preilluminated leaves, respectively. A Schott KL-1500 lamp was used as the actinic light source, with an intensity of 300 μmol photons m^{-2} s^{-1}. The measurements were performed on leaves that were dark adapted for at least 30 min.

State transitions were measured essentially as described by Lunde et al. (2000). The far-red light (state 1) was provided by a Waltz 102 FR lamp, and state 2 was induced by blue light from a Schott KL-1500 lamp equipped with a Corning 4-96 filter (120 μmol photons m^{-2} s^{-1}). A weak light pulse was given in order to predict F_0, and subsequently, a saturating flash of 6,000 μmol photons m^{-2} s^{-1} was given for 800 ms in order to determine F_m. The leaf was equilibrated with blue light for approximately 20 min until stable F_{ii}' (fluorescence without PSI light) levels were attained (state 2). A second saturating flash of white light was given to predict F_{m2}, and immediately thereafter, red light was added for 20 min to bring the leaf to state 1. Then, a third pulse of white light was given to predict F_{m1}. The red light was turned off, and after 20 min the blue light also was switched off and F_0' could be determined. State transitions were determined using the change in F_m in each of the states, based on the assumption that the light intensity used to induce state transitions was insufficient to cause photoinhibition. This being so, the difference in F_m was due to state transitions and can be expressed as a percentage change $[(F_{m1} - F_{m2})/F_{m1}]$; Bellafiore et al., 2005). Special care was taken to prevent photoinhibition during measurements by avoiding supersaturating light conditions. It was ensured that the baseline fluorescence during measurements was stable and that no significant curvature occurred over time, indicating stable analytical conditions and accurate state transition measurements.

Chl Analysis

Total Chl was determined by methanol extraction of the youngest fully expanded leaf according to the method of Lichtenthaler and Wellburn (1983). The Chl content was determined by UV spectroscopy (U-2000; Hitachi).

Immunoblotting

Thylakoid membranes were extracted 55 d after planting and used for immunoblotting. Twenty micrograms of total thylakoid proteins was separated by SDS-PAGE and transferred to a nitrocellulose membrane by blotting as reported previously (Jensen et al., 2000). An internal thylakoid control sample was run on each gel and afterward used to correct the gels for unequal blotting. CF1-ATPase was used as a loading control to demonstrate equal loading of proteins, and a Coomassie Brilliant Blue-stained gel was used to enable quantification of specific proteins per unit loaded protein. All antibodies were obtained from Agrisera. Immunoblotting analysis of each preparation was repeated two or three times, and generally the results varied by 20% to 30%. Primary antibodies were detected using a chemiluminescent detection system (Super-Signal; Pierce) according to the instructions of the manufacturer. The chemiluminescent signal produced was recorded digitally using a cooled CCD camera with the AC1 AutoChemi System (Ultra-Violet Products). The exposure time was set to 5 min, with accumulative snapshots at 30-s intervals. Signal intensity was quantified using the LabWorks Analysis Software (Ultra-Violet Products).

Data Analysis

Statistical analysis was undertaken using SAS (SAS Institute; version 8.2) for variance analysis and Student's *t* test for comparison of means. Mean values (X) are listed with the associated SE values ($X \pm SD/\sqrt{n}$).

ACKNOWLEDGMENTS

The skillful assistance of Bente Broeng with ICP-MS and Lis Drayton Hansen with immunoblotting analysis are gratefully acknowledged.

Received December 18, 2008; accepted April 4, 2009; published April 15, 2009.

LITERATURE CITED

Allen J, Bennett J, Steinback K, Arntzen C (1981) Chloroplast protein phosphorylation couples plastoquinone redox state distribution of excitation energy between photosystems. Nature **291:** 25–29

Anderson JM, Boardman NK, David DJ (1964) Trace metal composition of fractions obtained by digitonin fragmentation of spinach chloroplasts. Biochem Biophys Res Commun **17:** 685–689

Anderson JM, Thorne SW (1968) The fluorescence properties of manganese deficient spinach chloroplasts. Biochim Biophys Acta **162:** 122–134

Andersson B, Pyliotis NA (1969) Studies with manganese-deficient spinach chloroplasts. Biochim Biophys Acta **189:** 280–293

Apel K, Hirt H (2004) Reactive oxygen species: metabolism, oxidative stress, and signal transduction. Annu Rev Plant Biol **55:** 373–399

Aro EM, Suorsa M, Rokka A, Allahverdiyeva Y, Paakkarinen V, Saleem A, Battchikova N, Rintamäki E (2005) Dynamics of photosystem II: a proteomic approach to thylakoid protein complexes. J Exp Bot **56:** 347–356

Aro EM, Virgin I, Andersson B (1993) Photoinhibition of photosystem II: inactivation, protein damage and turnover. Biochim Biophys Acta **1143:** 113–134

Ascher-Ellis JS, Graham RD, Hollamby GJ, Paull J, Davies P, Huang C, Pallotta MA, Howes N, Khabaz-Saberi H, Jefferies SP, et al (2001): Micronutrients. *In* MP Reynolds, JI Ortiz-Monasterio, A McNab, eds,

Application of Physiology in Wheat Breeding. International Maize and Wheat Improvement Center, El Batan, Mexico, pp 219–240

Barber J (2004) Towards a full understanding of water splitting in photosynthesis. International Journal of Photoenergy **6:** 43–51

Bellafiore S, Barneche F, Peltiers G, Rocahix JD (2005) State transitions and light adaptation require chloroplast thylakoid protein kinase STN7. Nature **433:** 892–895

Björkman O, Demmig B (1987) Photon yield of O_2 evolution and chlorophyll fluorescence characteristics at 77 K among vascular plants of diverse origins. Planta **170:** 489–504

Bromfield SM (1958) The solution of MnO_2 by substances released from soil and from the roots of oats and vetch in relation to manganese availability. Plant Soil **10:** 147–160

Bukhov NG, Egorova EA, Gvindachary S, Carpentier R (2004) Changes in polyphasic chlorophyll a fluorescence induction curve upon inhibition of donor or acceptor side of photosystem II in isolated thylakoids. Biochim Biophys Acta **1657:** 121–130

Chatterjee C, Nautiyal N, Agarwala SC (1994) Influence of changes in manganese and magnesium supply on some aspects of wheat physiology. Soil Sci Plant Nutr **40:** 191–197

Dasgupta J, Ananyev GM, Dismukes GC (2008) Photoassembly of the water-oxidizing complex in photosystem II. Coord Chem Rev **252:** 347–360

Haldrup A, Jensen PE, Lunde C, Scheller HV (2001) Balance of power: a view of the mechanism of photosynthetic state transitions. Trends Plant Sci **6:** 301–305

Hannam RJ, Graham RD, Riggs JL (1985) Diagnosis and prognosis of manganese deficiency in *Lupinus angustifolius* L. Aust J Agric Res **36:** 765–777

He Q, Vermaas W (1998) Chlorophyll a availability affects PsbA translation and D1 precursor processing in vivo in Synechocystis sp. PCC 6803. Proc Natl Acad Sci USA **95:** 5830–5835

Hebbern CA, Holst Laursen K, Ladegaard AH, Schmidt SB, Pedas P, Bruhn D, Schjoerring JK, Wulfsohn D, Husted S (2009) Latent manganese deficiency increases transpiration in barley (*Hordeum vulgare* L.). Physiol Plant **135:** 307–316

Hebbern CA, Pedas P, Schjoerring JK, Knudsen L, Husted S (2005) Genotypic differences in manganese efficiency: a field trial with winter barley (*Hordeum vulgare* L.). Plant Soil **272:** 233–244

Hill R, Larkum AWD, Frankart C, Kuhl M, Ralph PJ (2004) Loss of functional photosystem II reaction centers in zooxanthellae exposed to bleaching conditions: using fluorescence rise kinetics. Photosynth Res **82:** 59–72

Husted S, Hebbern CA, Mattsson M, Schjoerring JK (2000) A critical experimental evaluation of methods for determination of NH_4^+ in plant tissue, xylem sap and apoplastic fluid. Physiol Plant **109:** 167–179

Husted S, Mikkelsen BF, Jensen J, Nielsen NE (2004) Elemental fingerprint analysis of barley (*Hordeum vulgare*) using inductively coupled plasma mass spectrometry, isotope-ratio mass spectrometry, and multivariate statistics. Anal Bioanal Chem **378:** 171–182

Jensen PE, Gilpin M, Knoetzel J, Scheller HV (2000) The PSI-K subunit of photosystem I is involved in the interaction between light-harvesting complex I and the photosystem I reaction center core. J Biol Chem **275:** 24701–24708

Jiang CD, Gao HY, Zou Q (2002) Characteristics of photosynthetic apparatus in Mn-starved maize leaves. Photosynthetica **40:** 209–213

Kok B, Forbush B, McGloin M (1970) Cooperation of charges in photosynthetic O_2 evolution. I. A linear four-step mechanism. Photochem Photobiol **11:** 467–475

Krause GH, Weis E (1991) Chlorophyll fluorescence and photosynthesis: the basics. Annu Rev Plant Physiol Plant Mol Biol **42:** 319–349

Kriedemann PE, Graham RD, Wiskich JT (1985) Photosynthetic dysfunction and in vivo changes in chlorophyll a fluorescence from manganese-deficient wheat leaves. Aust J Agric Res **36:** 157–169

Krieger A, Rutherford AW, Vass I, Hideg E (1998) Relationship between activity, D1 loss, and Mn binding in photoinhibition of photosystem II. Biochemistry **37:** 16262–16269

Lazar D (2006) The polyphasic chlorophyll a fluorescence rise measured under high intensity of exciting light. Funct Plant Biol **33:** 9–30

Lichtenthaler HK, Wellburn AR (1983) Determinations of total carotenoids and chlorophylls a and b of leaf extracts in different solvents. Biochem Soc Trans **11:** 591–592

Lunde C, Jensen PE, Haldrup A, Knoetzel J, Scheller HV (2000) The PSI-H subunit of photosystem I is essential for state transitions in plant photosynthesis. Nature **408:** 613–615

Lunde C, Jensen PE, Rosgaard L, Haldrup A, Gilpin MJ, Scheller HV (2003) Plants impaired in state transitions can to a large degree compensate for their defect. Plant Cell Physiol **44:** 44–54

Møller IM, Jensen PE, Hansson A (2007) Oxidative modifications to cellular components in plants. Annu Rev Plant Biol **58:** 549–581

Muller P, Xiao-Ping L, Niyogi K (2001) Non-photochemical quenching: a response to excess light energy. Plant Physiol **125:** 1558–1566

Mullineaux CW, Emlyn-Jones D (2004) State transitions: an example of acclimation to low-light stress. J Exp Bot **56:** 389–393

Munday JC, Govindjee (1969) Light induced changes in the fluorescence yield of chlorophyll a in vivo. III. The dip and the peak in the fluorescence transient of chlorella pyrenoidosa. Biophys J **9:** 1–21

Nable RO, Bar-Akiva A, Loneragan JF (1984) Functional manganese requirement and its use as a critical value for diagnosis of manganese deficiency in subterranean clover (Triticum subterraneum L. cv. Seaton Park). Ann Bot (Lond) **54:** 39–49

Nixon PJ, Barker M, Boehm M, de Vries R, Komenda J (2004) FtsH-mediated repair of the photosystem II complex in response to light stress. J Exp Bot **56:** 357–363

Niyogi K, Shih C, Chow W, Pogson B, DellaPenna D, Björkman O (2001) Photoprotection in a zeaxanthin- and lutein-deficient double mutant of Arabidopsis. Photosynth Res **67:** 139–145

Papadakis IE, Bosabalidis AM, Soiropoulos TE, Therios IN (2007) Leaf anatomy and chloroplast ultrastructure of Mn-deficient orange plants. Acta Physiol Plant **29:** 297–301

Pearson JN, Rengel Z (1997) Genotypic differences in the production and partitioning of carbohydrates between roots and shoots of wheat grown under zinc or manganese deficiency. Ann Bot (Lond) **80:** 803–808

Pedas P, Hebbern CA, Schjoerring JK, Holm P, Husted S (2005) Differential capacity for high-affinity manganese uptake contributes to differences between barley genotypes in tolerance to low manganese availability. Plant Physiol **139:** 1411–1420

Pedas P, Ytting CK, Fuglsang AT, Jahn TP, Schjoerring JK, Husted S (2008) Manganese efficiency in barley: identification and characterization of the metal ion transporter HvIRT1. Plant Physiol **148:** 455–466

Rengel Z (1997) Root exudation and microflora populations in rhizosphere of crop genotypes differing in tolerance to micronutrient deficiency. Plant Soil **196:** 255–260

Reuter DJ, Edwards DG, Wilhelm NS (1997) Temperate and tropical crops. *In* DJ Reuter, JB Robinson, eds, Plant Analysis: An Interpretation Manual, Ed 2. CSIRO Publishing, Victoria, Australia, pp 81–279

Rosenqvist E, van Koten O (2003) Chlorophyll fluorescence: a general description and nomenclature *In* JR Dell, PMA Toivonen, eds, Practical Applications of Chlorophyll Fluorescence in Plant Biology. Kluwer Academic Publishers, London, pp 32–77

Simpson DJ, Robinson SP (1984) Freeze-fracture ultrastructure of thylakoid membranes in chloroplasts from manganese-deficient plants. Plant Physiol **74:** 735–741

Srivastava A, Guisse B, Greppin H, Strasser R (1997) Regulation of antenna structure and electron transport in photosystem II of Pisum sativum under elevated temperature probed by the fast polyphasic chlorophyll a fluorescent transient OKJIP. Biochim Biophys Acta **1320:** 95–106

Strasser RJ (1997) Donor side capacity of photosystem II probed by chlorophyll a fluorescent transients. Photosynth Res **52:** 147–155

Strasser RJ, Srivastava A, Govindjee (1995) Polyphasic chlorophyll *a* fluorescence transients in plants and cyanobacteria. Photochem Photobiol **61:** 32–42

Strasser RJ, Tsimilli-Michael M, Srivastava A (2004) Analysis of the chlorophyll *a* fluorescence transient. *In* GC Papageorgiou, Govindjee, eds, Advances in Photosynthesis and Respiration: Chlorophyll a Fluorescence. A Signature of Photosynthesis. Springer, Dordrecht, The Netherlands, pp 321–362

Yang XE, Chen WR, Feng Y (2007) Improving human micronutrient nutrition through biofortification in the soil-plant system: China as a case study. Environ Geochem Health **29:** 413–428